Comparison of the Monte Carlo simulation and the hypernetted-chain theory for the one-dimensional strongly coupled plasma

1985 J. Phys. A: Math. Gen. 18 3463

(http://iopscience.iop.org/0305-4470/18/17/029)

J. Phys. A: Math. Gen. 18 (1985) 3463-3469. Printed in Great Britain

COMMENT

Comparison of the Monte Carlo simulation and the hypernetted-chain theory for the one-dimensional strongly coupled plasma

Y Furutani, Y Oda† and H Totsuji

Department of Electronics, Okayama University, 3-1-1 Tsushimanaka, 700 Okayama, Japan

Received 20 December 1984

Abstract. The Monte Carlo simulation for the one-dimensional one-component plasma model is carried out. We obtain the pair distribution function $g_2(x)$ of a periodic structure, confirming the Kunz prediction that the one-dimensional one-component plasma remains in a crystalline state for any value of the plasma parameter. The Monte Carlo results are then compared with those obtained from the hypernetted-chain equation. Although the correlation energies calculated from the two approaches agree fairly well, the hypernetted chain $g_2(x)$ never reproduces the periodic structure, demonstrating that this scheme does not apply to a crystalline state.

1. Introduction

The classical one-component plasma (OCP) model composed of charged sheets which interact through the one-dimensional (1D) Coulomb ponteital $-e|x|$, with e the electronic charge and crossover among themselves in the direction normal to their plane, had already been exploited two decades ago by Buneman (1959) and Dawson (1962) to investigate large-amplitude electron plasma oscillations. Statistical mechanics of such an OCP has been fully discussed by several authors (Lenard 1961, Edwards and Lenard 1962, Baxter 1964, Kunz 1974, Choquard *et al* 1981). In particular, Kunz predicts that the 1D OCP remains in a crystalline state for any value of the 1D plasma parameter $\Lambda\ (=\beta e^2\lambda_D)$, in that thermodynamic functions such as pressure have no singularity and the 1D OCP does not undergo any phase transition. Here, $\beta=(k_BT)^{-1}$ and λ_D represents the 1D Debye length $(2\beta\rho e^2)^{-1/2}$. Other notation is customary.

On our side, we have long concentrated on the study of nodal expansions for a strongly coupled OCP, in view to elucidating the role of irreducible (bridge) graphs in three dimensions in the hypernetted-chain (HNC) approximation (Deutsch *et al* 1976, 1981). In this respect, we should recall recent impressive efforts for improving the usual HNC scheme which assert that a family of bridge graphs gives a substantial contribution to the behaviour of the pair distribution function $g_2(x)$ in the short and intermediate ranges (Rosenfeld and Ashcroft 1979, Iyetomi and Ichimaru 1982, 1983).

From the viewpoint of the nodal expansion, however, analysis of the simplest bridge graph of the third order in plasma parameter is hardly tractable in three

† Present address: Department of Solid-State Physics, Faculty of Science, Hiroshima University, 730 Hiroshima, Japan.

0305-4470/85/173463+07$02.25

dimensions (Cohen and Murphy 1969, Furutani *et al* 1981). The 1D OCP offers a fortunate situation for this circumstance, since any bridge graph at least of the third and fourth orders in Λ and their resummed descendents can be evaluated analytically, which may then be used to check to what accuracy the nodal expansion approximation could reproduce the MC data. We thus find it necessary to carry out the MC run for the 1D OCP as a preliminary of the HNC equation study of a potential of average force $w_2(x)$, in which resummed reducible and bridge graphs of the third order in Λ are all incorporated.

The purpose of this comment is to present the MC data and compare them with the routine HNC results which exclude completely, as a first rough approximation, any contribution of bridge graphs. Thorough study of these single-bonded and resummed reducible and bridge graphs and their contribution to $g_2(x)$ will be discussed in a separate paper. The comment is organised thus. In § 2, we derive an expression for the correlation energy, used to carry out the Monte Carlo (MC) run. In § 3, the HNC scheme transcribed to the 1D OCP is briefly explained. Finally, concluding remarks which include the comparison of the correlation energy obtained from two different approaches are given in § 4.

2. MC simulation

In order to evaluate the correlation energy of an infinite system, we divide the total system into a number of periodic unit cells, each including several tens of charged sheets. Assuming a rigid uniform background of opposite charge, the correlation energy $v(x_{ij})$ between the ith sheet at x_i and the jth sheet at x_j and its images is given by

$$v(x_{ij}) = \frac{2e^2}{L_0}\sum_K{}' \frac{1}{K^2}\exp(\mathrm{i}Kx_{ij}) = \frac{e^2}{4L_0}\left((2x_{ij}-L_0)^2 - \frac{L_0^2}{3}\right), \tag{1}$$

$KL_0 = 2\pi m$, $m = 0, \pm 1, \pm 2, \ldots$ and $x_{ij} = |x_i - x_j|$. Here, L_0 is the length of the unit cell which we take later as unity and K the reciprocal lattice vector. The prime indicates that the $K = 0$ contribution is deleted from the sum. This is the 1D analogue of the 2D MC simulation exploited by one of us (Totsuji 1978). Then, the total correlation energy between the ith sheet and the jth sheet and its images can be written as

$$\frac{2e^2}{L_0}\sum_n\sum_K{}' \frac{1}{K^2}\exp[\mathrm{i}K(x_{ij} - nL_0)] \tag{2}$$

with $n = 0, \pm 1, \pm 2, \ldots$. Since $v(x_{ij})$ is periodic with period L_0, the correlation energy per unit cell between the sheets ij and their images is given by $v(x_{ij})$. The correlation energy of the unit cell is then calculated, by virtue of (1), as

$$U = \sum_{1 \le i < j \le N_0} v(x_{ij}) + \tfrac{1}{2}N_0 U_{\mathrm{M}} \tag{3}$$

with N_0 the number of sheets within the unit cell and U_{M} the Madelung energy. Evaluating (3) explicitly, we obtain the correlation energy, normalised by the total thermal energy of sheets in the unit cell, which reads as

$$U_{\mathrm{N}} = \frac{U}{N_0 k_{\mathrm{B}} T} = 2\Lambda^2\left((N_0-1)\sum_{i=1}^{N_0} x_i^2 - 2\sum_{i=2}^{N_0} x_i \sum_{j=1}^{i-1} x_j - \sum_{i=1}^{N_0}(2i-1-N_0)x_i + \tfrac{1}{12}N_0^2\right) \tag{4}$$

Here the sheets are numbered so that $x_j > x_i$ when $j > i$ and L_0 is taken as unity. This is the expression we have utilised for the MC simulation. Though it remains to prove that U_N is independent of N_0, we have confirmed numerically that choice of two different N_0 values does not affect U_N, as indicated in table 1.

Table 1. Effect of N_0 on $U_N^{(MC)}$ for $\Lambda = 4$ and 10.

N_0 \ Λ	4	10
16	3.120 ± 0.050	17.05 ± 0.08
32	3.126 ± 0.056	16.99 ± 0.06

The behaviour of $g_2(x)$ for three different Λ values is illustrated in figure 1. As was already mentioned in § 1, the rigorous Baxter-Kunz theory predicts the 1D OCP to exhibit a crystalline structure (Wigner lattice), in the asymptotic domain, for any value of Λ, as small as it is. This general trend is clearly demonstrated by the MC $g_2(x)$: (1) the spacing of two adjacent peaks coincides with the mean separation $a(=1/N_0)$ between sheets and (2) a finite train of peaks with the same amplitude are observed within the cell. The values of U_N evaluated from (4) for about a million of steps in the MC run are shown in the second column of table 2, in view of comparison with those obtained from the HNC U_N.

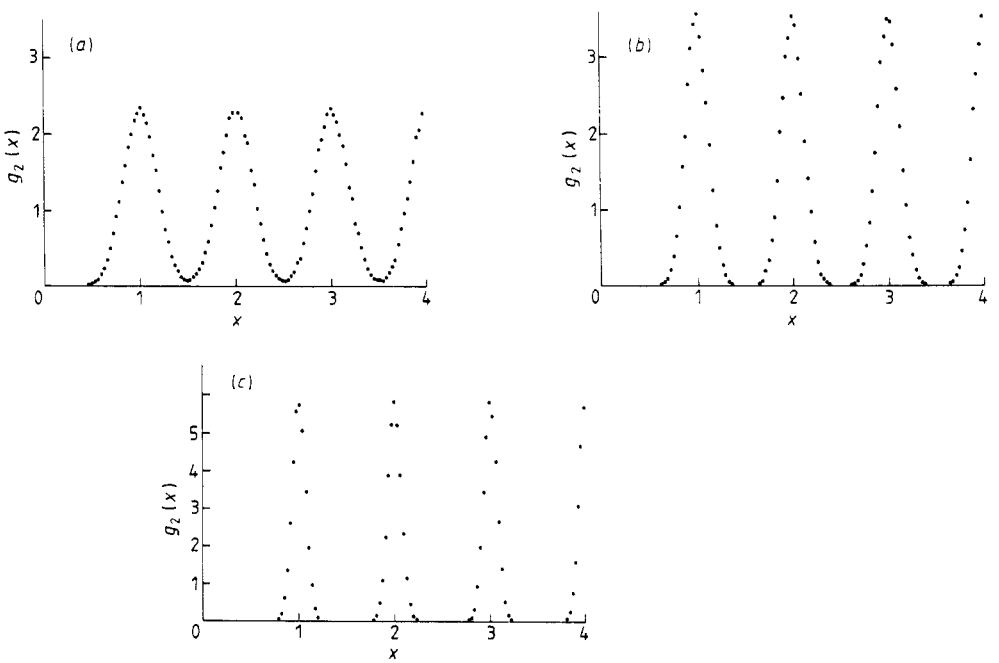

Figure 1. The MC $g_2(x)$ as a function of the distance in units of the mean separation between sheets are illustrated for three different Λ values: $\Lambda = 4$ in (a), $\Lambda = 6$ in (b) and $\Lambda = 10$ in (c).

Table 2. Normalised correlation energy against Λ. $U_N^{(MC)}$ and $U_N^{(HNC)}$ are obtained from (4), the MC formula, and (7), the HNC relation.

Λ	$U_N^{(MC)}$	$U_N^{(HNC)}$
1		0.5246
2	1.093 ± 0.108	1.199
3		2.123
4	3.126 ± 0.056	3.353
5		4.899
6	6.398 ± 0.011	6.776
8		11.50
10	16.99 ± 0.06	17.52

3. HNC calculation

We next evaluate $g_2(x)$ as a solution to the 1D HNC equation, in which no bridge contribution is retained. Defining the potential of average force $w_2(x)$ as $w_2(x) = \ln g_2(x)$, we have a well known set of equations

$$w_2(x) = -\Lambda \exp(-|x|/\lambda_D) + S(x) \tag{5a}$$

$$G(x) = \exp(w_2(x)) - 1 - w_2(x) \tag{5b}$$

$$\tilde{S}(k) = \frac{(k\lambda_D)^2}{1+(k\lambda_D)^2} \frac{\tilde{G}(k)}{1+(k\lambda_D)^{-2} - \tilde{G}(k)} - \tilde{G}(k) \tag{5c}$$

where $\tilde{G}(k)$ and $\tilde{S}(k)$ are the Fourier transform of $G(x)$ and $S(x)$, respectively. $S(x)$ defines the departure of $w_2(x)$ not from the bare 1D Coulomb potential $-\Lambda|x|/\lambda_D$ but from the screened 1D Debye potential $-\Lambda \exp(-|x|/\lambda_D)$, the usual procedure we have utilised in the study of the nodal expansion (Deutsch *et al* 1976, 1981). Our HNC iteration procedure is summarised as follows. Let $S_i(x_n)$ and $S_0(x_n)$ be an iteration input and output of $S(x)$ at $x = x_n$ and $\Delta x = x_{n+1} - x_n$. Iteration starts with the initial guess $S_i(x_n) = 0$. After the first iteration for a set of coordinates $x_n (n = 1, 2, \ldots, n_{max})$, we obtain the output $S_0(x_n)$. With the aid of the extrapolation relation for the $(\nu+1)$th input $S_i^{(\nu+1)}(x_n)$:

$$S_i^{(\nu+1)}(x_n) = \alpha S_0^{(\nu)}(x_n) + (1-\alpha) S_i^{(\nu)}(x_n)$$

we can continue the iteration, where α is an extrapolation parameter properly chosen so as to accelerate the convergency. At the end of each iteration, we check the convergency by the criterion

$$\left(\sum_{i=1}^{n_{max}} \{S_i(x_n) - S_0(x_n)\}^2 \Delta x \right)^{1/2} < \varepsilon. \tag{6}$$

If, after the νth iteration, the above inequality is satisfied, iteration stops. Figure 2 shows the HNC $g_2(x)$ for different Λ values. It makes clear that the HNC $g_2(x)$ behaves, unlike the MC one, as a damped oscillation about unity, with several peaks located at the corresponding lattice points. As a reference, we tabulate, at the third column of

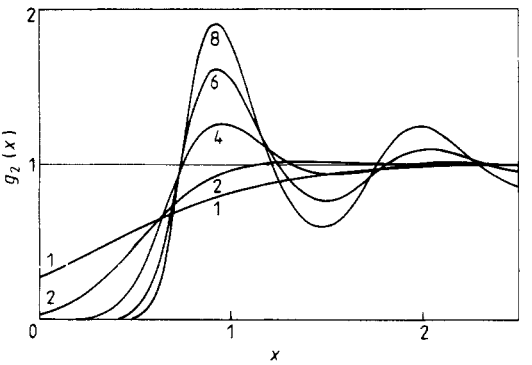

Figure 2. The HNC $g_2(x)$ as a function of the distance. The normalisation is the same as in figure 1. Numbers on the curves represent the Λ values.

table 2, the values of U_N calculated from the HNC $g_2(x)$ via the relation

$$U_N^{(HNC)} = -\frac{2\Lambda^2}{a^2}\int_0^\infty dx\, x[g_2^{(HNC)}(x)-1]. \tag{7}$$

We also illustrate the exact Baxter-Kunz U_N, our MC $U_N^{(MC)}$ and the corresponding $U_N^{(HNC)}$ in figure 3 as a function of Λ. The fact that $U_N^{(HNC)}$ slightly exceeds $U_N^{(MC)}$

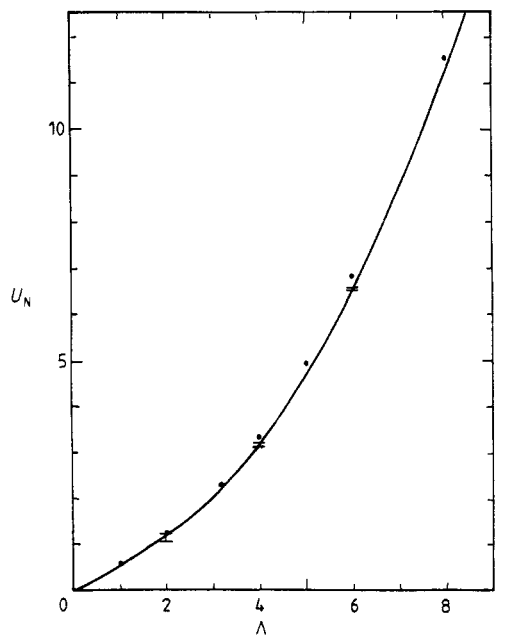

Figure 3. Normalised correlation energy evaluated from the HNC iteration and the MC simulation, in comparison with the exact Baxter-Kunz result depicted by the full curve (after Totsuji 1979). The bar indicates the MC result, while the circle represents the HNC value.

does not preclude that the former stands legitimately in its own right, since the correlation energy is a smeared-out quantity by integration over x. In this respect, the comparison of two U_N has little physical meaning.

4. Concluding remarks

So far we have given the results for $g_2(x)$ and U_N obtained from two different approaches, the MC simulation and the HNC equation. In contradistinction to a satisfactory agreement between $U_N^{(MC)}$ and $U_N^{(HNC)}$, the behaviour of $g_2^{(HNC)}(x)$ differs substantially from $g_2^{(MC)}(x)$: while the MC $g_2(x)$ reveals the crystalline structure, confirming apparently the Kunz prediction, the HNC $g_2(x)$ manifests a damped oscillation, characteristic of a pair distribution function for a liquid. It is time to explain the origin of this discrepancy. As was briefly touched upon in § 1, serious effort for improving the 3D $g_2(x)$ by inclusion of a family of bridge graphs, important in the short and intermediate ranges, has been successful (Rosenfeld and Ashcroft 1979, Iyetomi and Ichimaru 1982, 1983). This is because a 3D plasma remains in a liquid phase below some critical Λ value and the HNC scheme works, since it reproduces at least qualitatively results of numerical experiments. On the other hand, application of the HNC equation to the 1D OCP, which is believed to be in a crystalline state, gives a wrong result, in that the HNC approach gives *always* a damped oscillation, irrespective of the dimensionality.

From the viewpoint of the nodal expansion, the essential ingredient of the HNC scheme is the longest convolution chains (Del Rio and De Witt 1969). It is thus of interest to study how the HNC result is modified by inclusion of the bridge contribution or by construction of a new set of equations based upon a so-called 'short-range resummation'. In this respect, we note that the 1D OCP offers a sole testing ground, in that evaluation of bridge graphs is mostly tractable in contrast to the 3D case. Finally, the problem of understanding whether the nodal expansion is applicable to a crystalline state or not, which is not yet proven until now at least to our knowledge, is left open for future study.

Acknowledgments

One of us (YF) is grateful to Professor S Ichimaru for helpful suggestions. Numerical work has been done at the Computer Center of Okayama University.

References

Baxter R 1964 *Phys. Fluids* **7** 38
Buneman O 1959 *Phys. Rev.* **115** 503
Choquard Ph, Kunz H, Martin Ph A and Navet M 1981 in *Physics in One Dimension* ed J Bernasconi and T Schneider (Berlin: Springer) p 335
Cohen E G D and Murphy T J 1969 *Phys. Fluids* **12** 1404
Dawson J M 1962 *Phys. Fluids* **5** 445
Del Rio F and De Witt H E 1969 *Phys. Fluids* **12** 791
Deutsch C, Furutani Y and Gombert M M 1976 *Phys. Rev.* A **13** 2244
—— 1981 *Phys. Rep.* **69** 85

Edwards S F and Lenard A 1962 *J. Math. Phys.* **3** 778
Furutani Y, Deutsch C and Oda Y 1981 *J. Physique Lett.* **42** L285
Iyetomi H and Ichimaru S 1982 *Phys. Rev.* A **25** 2434
—— 1983 *Phys. Rev.* A **27** 3241
Kunz H 1974 *Ann. Phys., NY* **85** 303
Lenard A 1961 *J. Math. Phys.* **2** 682
Rosenfeld Y and Ashcroft N W 1979 *Phys. Rev.* A **20** 1208
Totsuji H 1978 *Phys. Rev.* A **17** 399
—— 1979 *Phys. Rev.* A **19** 2433